International Journal of Research in Engineering and Innovation (IJREI)
journal home page: http://www.ijrei.com
ISSN (Online): 2456-6934

ORIGINAL ARTICLE

Effect of processing parameters on the mechanical properties and microstructure of the dissimilar aluminum alloys of AA7475 and AA6061

Vasim Abbas, Gaurav Kumar, Mukesh kumar

Department of Mechanical Engineering, Vidya College of Engineering, Meerut, India

Article Information

Received: 24 January 2022
Revised: 21 February 2022
Accepted: 27 February 2022
Available online: 05 March 2022

Keywords:

Friction stir welding
Microhardness
Microstructure
Tensile strength
Tool rotational speed (TRS)

Abstract

Friction stir welding (FSW) is widely used in automobile and aerospace industries to join light metal through higher plastic deformation rates. Because joining of dissimilar light metal is very difficult to join via fusion welding
In this work, the friction stir welding (FSW) was successfully fabricate to join dissimilar aluminum alloys of AA7475 and AA6061, and revealed that tensile strength and hardness increased with increasing tool rotation. The maximum tensile strength and the % strain at SZ were observed 247.41 MPa and 18.24%at TRS 1200 rpm and TS 105 mm/min, respectively, and the higher microhardness (127 HV) at SZ was perceived at TRS 1000 rpm and TS 90 mm/min. The microstructure in the stir zone was substantially finer with higher tool rotation than the low TRS. The big and deep dimples can be seen in the FSWed part at 1000 rpm, whereas equiaxed fine dimples can be seen at TRS of 1200 rpm.

1. Introduction

The FSW was developed by The Welding Institute in the UK in December 1991 that was a solid-state joining technique for light material i.e. magnesium and aluminum alloys that are used in automobile production industries, aerospace engineering, and transportation industries [1, 2] shown in fig. 1. This technique might be employed to create a sound junction in aluminum alloys (Al-alloys) [3, 4]. During this process, the traverse speed (TS) welded joint, rotational tool speed (TRS), and pin geometry all have a vital role in analyzing material plasticization around the rotating tool pin, Numerous work has been published in similar and dissimilar aluminum and light metal alloys [5, 6] due to its potential to decrease local casting defect, microvoids, welding defects of the traditional fusion process. Welding of various aluminum or light metal alloys using fusion welding is very difficult to join due to their varying thermal properties, mechanical and chemical properties. Based on the aforementioned, the FSE is a very useful welding process for removing the welding defects in light metal alloys. Various investigators have successfully fabricated dissimilar and bimetallic welded joints via FSW and analyzed the mechanical behavior of the welded region [7]. Guo et al. [8] reported that welding at a high speed resulted in the strongest joint. A new welding technique was presented to increase the welding efficiency of TIG joints. The effect of the friction stir process on TIG welded joints was investigated, and mechanical features and temperature distribution of the TIG+FSP joints were revealed [9-15]. Because of high corrosion resistance, superior machinability, and high strength-to-weight ratio, light metal alloys are used for marine, aerospace, and automobile engineering [16]. Standard fusion welding processes, on the other hand, are known to be problematic for joining Al alloys [17], with some of these

Corresponding author: Gaurav Kumar
Email Address: gaurav.me86@gmail.com
https://doi.org/10.36037/IJREI.2022.6108

concerns being the formation of residual stress, severe deformation, solidification, and secondary brittle phases.

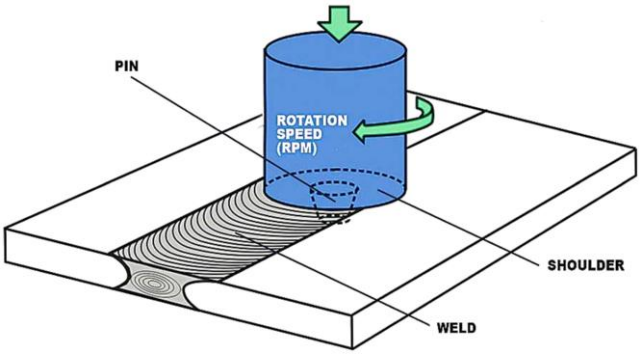

Figure 1: Schematic diagram of FSW

The heat-treatable Al-alloys like the 6XXX and 7XXX series [16] are among the most complex and widely used in the automobile and aerospace industries. The AA6061 series of materials are frequently utilized in aircraft, storage tanks, pipelines, and marine frames [18]. In contrast, the 7XXX series alloys have high corrosion and toughness resistance [19]. These Al-alloys are reinforced by artificial aging and heat treatment to produce hard Mg_2Si precipitates [20-22]. Although normal fusion joining process may weld the AA6061, traditional processes deem the AA7050 alloy "unweldable" [23]. However, several tests have also shown that FSW is effective for merging the AA6061 [24-27] and AA7050 [28, 29].

2. Materials and Methods

The FSWed joints were fabricated utilizing 6 mm thick rolled AA6061 and AA7475 plates. Table 1 summarizes the chemical compositions of both materials. The Al-alloys were fused at three different TRS ranging from 1000 to 1200 rpm, with the transverse speed fixed at 90-120 mm/min. The process parameters were selected using design expert software. Experiments were carried out on the FSW of AA7475 and AA6061 Al-alloys utilizing H13 tool steel of 6 mm diameter and 5.5 mm length of a square pin with shoulder diameters of 19 mm reveals in fig. 2. Following the completion of the welding, the bottom and top regions of FSWed joints were machine to have a smooth surface.

Table 1: Chemical composition of Al-alloys

Material	Si	Cu	Fe	Zn	Mg	Cr	Ti	Al
AA6061	0.7	0.2	0.6	0.3	0.8	0.2	0.15	Bal.
AA7475	0.05	1.9	0.08	5.8	2.3	0.05	0.03	Bal.

The upper surface of the parent metal observed flash material as a result of interaction between tool shoulder and the base plates that has been swirling and extruded around the pin. The specimens were then machined perpendicular to the welding direction for mechanical and microstructural characterization. The microstructures of the welds were studied using optical microscopy, and SEM analysis. The ASTM E8 standard was used to create the transverse sections of the weldment. Vickers hardness measurement were conducted on the FSWed samples' transverse cross-sections. At room temperature, tensile testing was done on the FSWed joints to characterize the tensile properties of the FSWed joints.

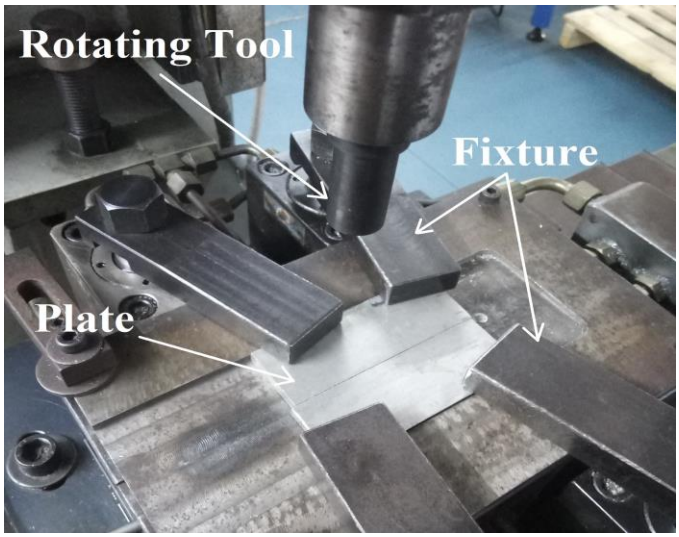

Figure 2: Experimental setup of FSW

3. Results and discussion

3.1 Ultimate Tensile strength (UTS)

The maximum joint efficiency of 85.02% was noticed at TRS of 1200 rpm, TS of 105 mm/min, and the least joint efficiency of 54.71% was noticed at TRS of 1100 rpm, TS of 120 mm/min demonstrated in table 2, since a lower TRS, results in a lower temperature dissemination, poor stirring action by the square pin, and observed insufficient consolidation of FSWed material by the tool shoulder [30]. As a result, the lowest joint efficiency or UTS was reported.

The heat input into the FSWed joint increased as the TRS increased, producing an ultrafine and equiaxed grain structure that improved tensile strength. When the TRS surpasses 1200 rpm, sufficient stirred welded material may be produced on the top surfaces of the parent metal, resulting in micro gaps in the SZ. Temperature increases, as well as grain coarsening and the rate of cooling at temperatures over the optimum temperature, may diminish the UTS of the welded region at high TRS. While the material flowed around the AS of the weldment, certain flaws were discovered [31]. The % strain of the welded junction was lower at 1000 rpm than at 1200 rpm shown in fig. 4. Fig. 3 depicts the tensile stress-strain diagram of FSWed joints with various processing conditions. The frictional heat was generated at low TRS by tool and parent metal will not have generated enough plasticized flow, resulting in deficiencies in the FSWed joints, while, the frictional heat is produced maximum temperature at low TS in the welded region, leading to additional heat flow in the weldment, resulting in flaws in the joints.

Table 2: Mechanical properties of FSWed joints of AA7475 and AA6061

Specimen No	TRS (rpm)	TS (mm/min)	UTS (MPa)	Joint efficiency (%)	Strain (%)	Microhardness at SZ (HV)
1	1000	120	207.12	71.18	17.82	116
2	1200	120	183.30	62.99	21.17	124
3	1100	120	159.21	54.71	15.45	108
4	1200	105	247.41	85.02	18.24	112
5	1100	90	178.67	61.40	17.06	114
6	1200	90	198.50	68.21	20.74	102
7	1000	90	209.87	72.12	19.22	127
8	1000	105	223.80	76.91	19.60	118
9	1100	105	234.11	80.45	22.90	120

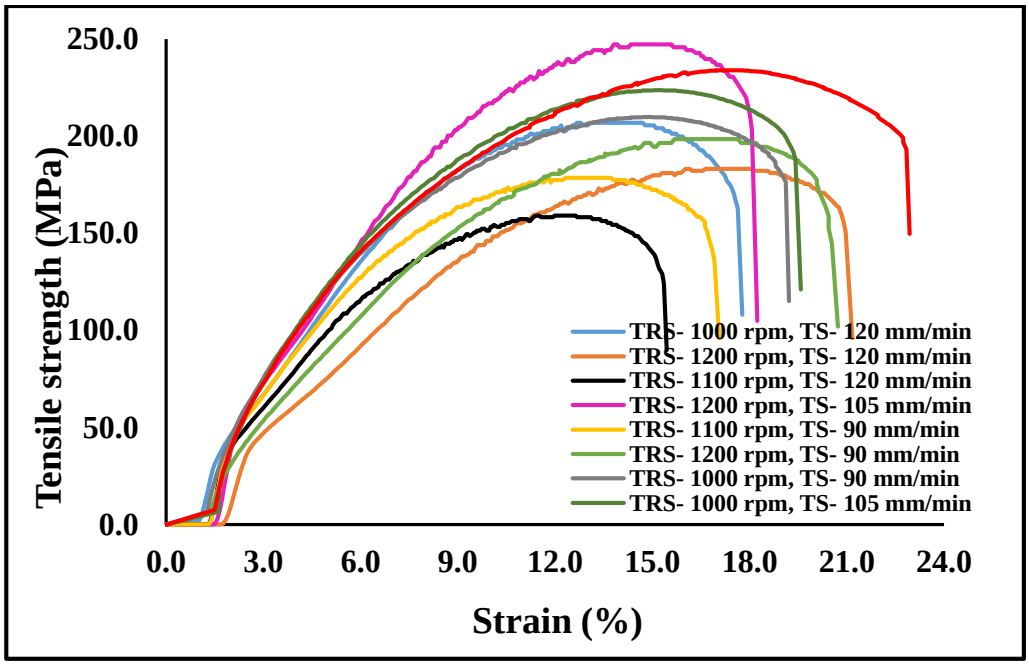

Figure 3: Comparison of stress-strain diagram of FSWed joint of AA AA7475 and AA6061 with different rotational speed

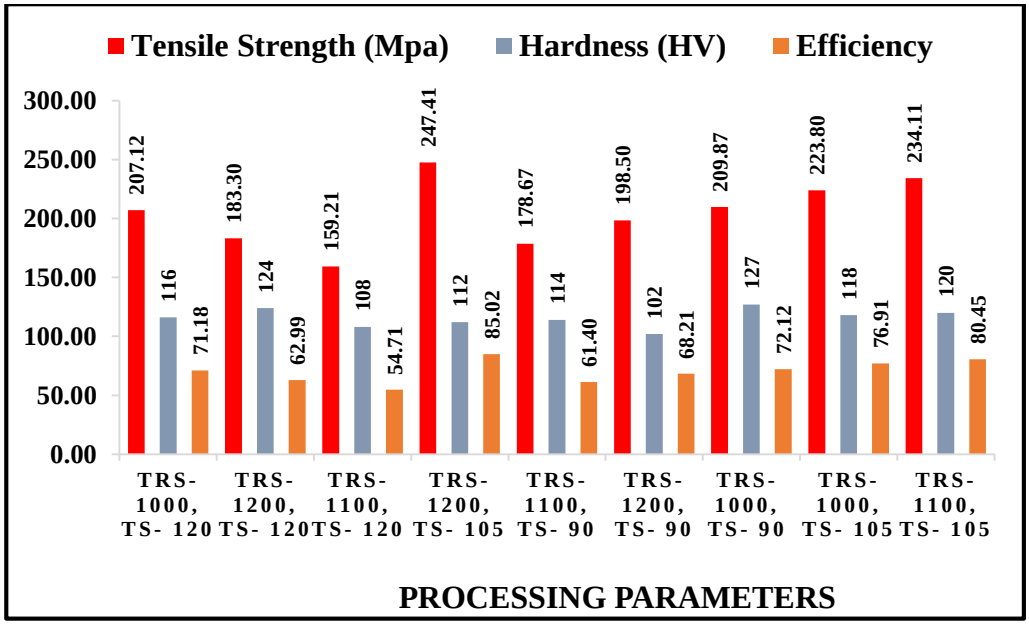

Figure 4: Variation of UTS and hardness to process parameters FSWed joint of AA AA7475 and AA6061

3.2 *Microhardness*

Presence of intermetallic compound, precipitates formation, and grain size all influence the microhardness of heat-treated Al-alloy FSW joints. As per the Hall-Petch correlation, the material hardness is inversely proportional to its grain size. Fine equiaxed grains formed by grain refinement caused by dynamic recrystallization in the SZ. Precipitate development, along with grain size has a significant effect on the tensile properties of the stir zone. The heat that was generated during friction between the tool and the base plate at the SZ soften the base metal, letting it flow freely around the tool pin and allowing for efficient material mixing, while also dissolving the strengthening precipitates, leading to hardness and strength losses. The maximum heat output is indispensable for optimal parent metal mixing and to avoid grain formation and precipitates dissolution. Grain formation and precipitate dissolution induce inferior microhardness in the HAZ and TMAZ of heat-treated Al-alloy FSWed joints. Because all joints are manufactured under identical FSW circumstances and both parent metal are age hardening Al-alloys, the grain size of SZ does not differ noticeably across all joints. The formation of precipitates has a substantial effect on the mechanical characterization of Al-alloys. The heat created during welding is felt by the SZ's adjacent regions (HAZ, TMAZ), resulting in hardness and strength loss. The strengthening precipitates present in the microstructure give strength to the precipitation hardening of AA7475 and AA6061. The distribution of strengthening precipitates was controlled by the temperature that the weld joint was subjected to different parameters. The heat generation in the HAZ and TMAZ of the joint induces the breakdown of the strengthening precipitates, resulting in lower hardness value in those areas. The relevant zones were softer as a result of precipitation disintegration. Because of precipitate coarsening and dissolution, lower hardness values have been reported at TMAZ and HAZ. The minimum hardness value in this study was reported at TRS of 1200 with TS of 90 mm/min, while the highest hardness value in the SZ was reported at TRS of 1000 rpm with TS of 90 mm/min shown in fig. 5.

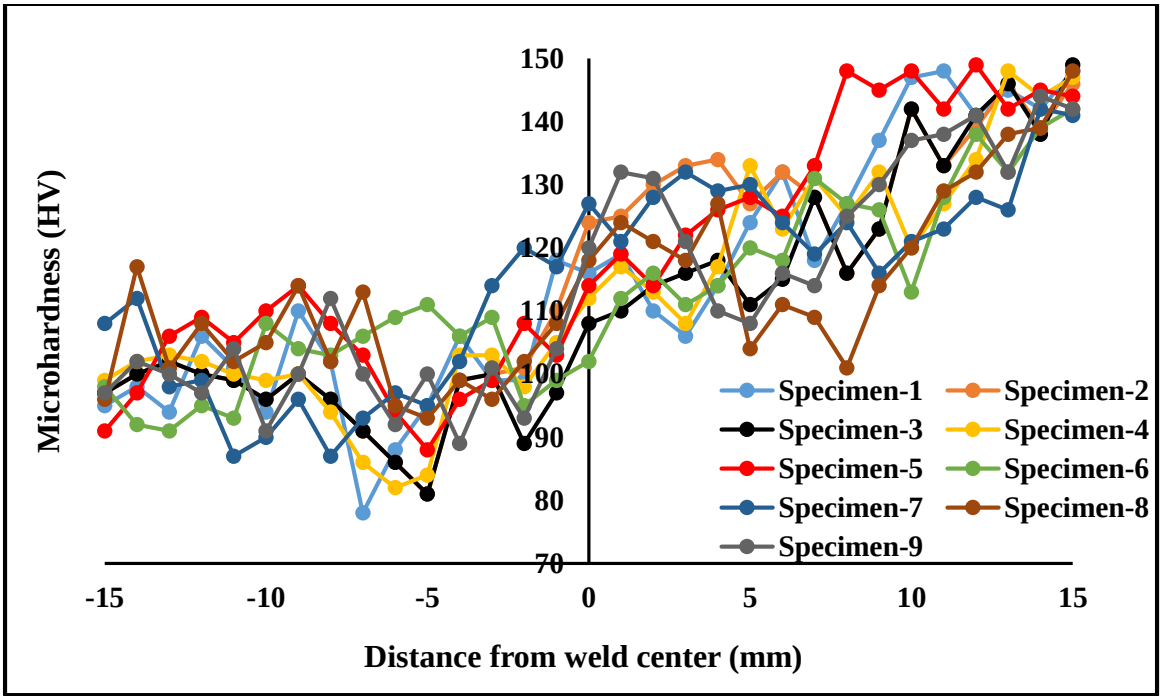

Figure 5: Distribution of micro-hardness of FSWed joint of AA7475 and AA6061 with different rotational speed

3.3 Microstructure observation

Fig. 6c depicts all of the weld zones, including the SZ, TMAZ, and base metal. The region where the tool shoulder acted can also be seen, which coincides with the junction of the top plate surface that delimits the SZ. The significantly different temperature and deformation related with these locations revealed that microstructure creation varies strongly with position and that this can occur both dynamically during the process and statically after [32, 33]. The mechanisms of microstructural evolution in dynamic recrystallization were investigated. The distinct zones are highlighted in Fig. 6, which depicts a typical profile of a linear friction weld. Detecting the boundary zone between the TMAZ and SZ on the indentation side is more difficult than on the feed side due to tool rotation and feed rate of the welding, which cause vortices and turbulence in this region. Furthermore, the micrograph in fig. 6 reveals the formation of concentric rings in the mixing zone, which is attributable to frictional heating caused by the tool's rotation and progress, which is capable of extruding the metal

that surrounds the pin towards the indentation side. There are damaged and elongated grains at this junction, indicating that they experienced moderate thermal cycle and plastic deformation [34-37]. The microstructure in the SZ region, which reveals the existence of fine grains due to recrystallized structure. Fig.6a-b demonstrate the microstructure of the parent metal, which has coarser granules as compared to the microstructure of the TMAZ, revealing a material that did not undergo plastic deformation or any heat cycling. Both AA7475 and AA6061 display strong plastic deformation at the SZ, leading in grain enhancement with a grain size of 9.2 µm at higher tool rotational speed and 21.52 µm at low rotational speed. Partially recrystallization was reported at the region of TMAZ due to inadequate distortion and lower temperature. The HAZ is the zone between both the TMAZ and the base metal that has only gone through the heat cycle and has not been subjected to plastic deformation [38, 39]. Because of the differences in the characteristics of the materials being welded, the microstructure in dissimilar joints consists of non-homogeneous plastic deformation. Results in heterogeneous material mixing and a reduction in joint strength [40]. Uneven heat distribution during FSW of different Al-alloys influences the tensile strength of the FSW joints reveals in fig. 7.

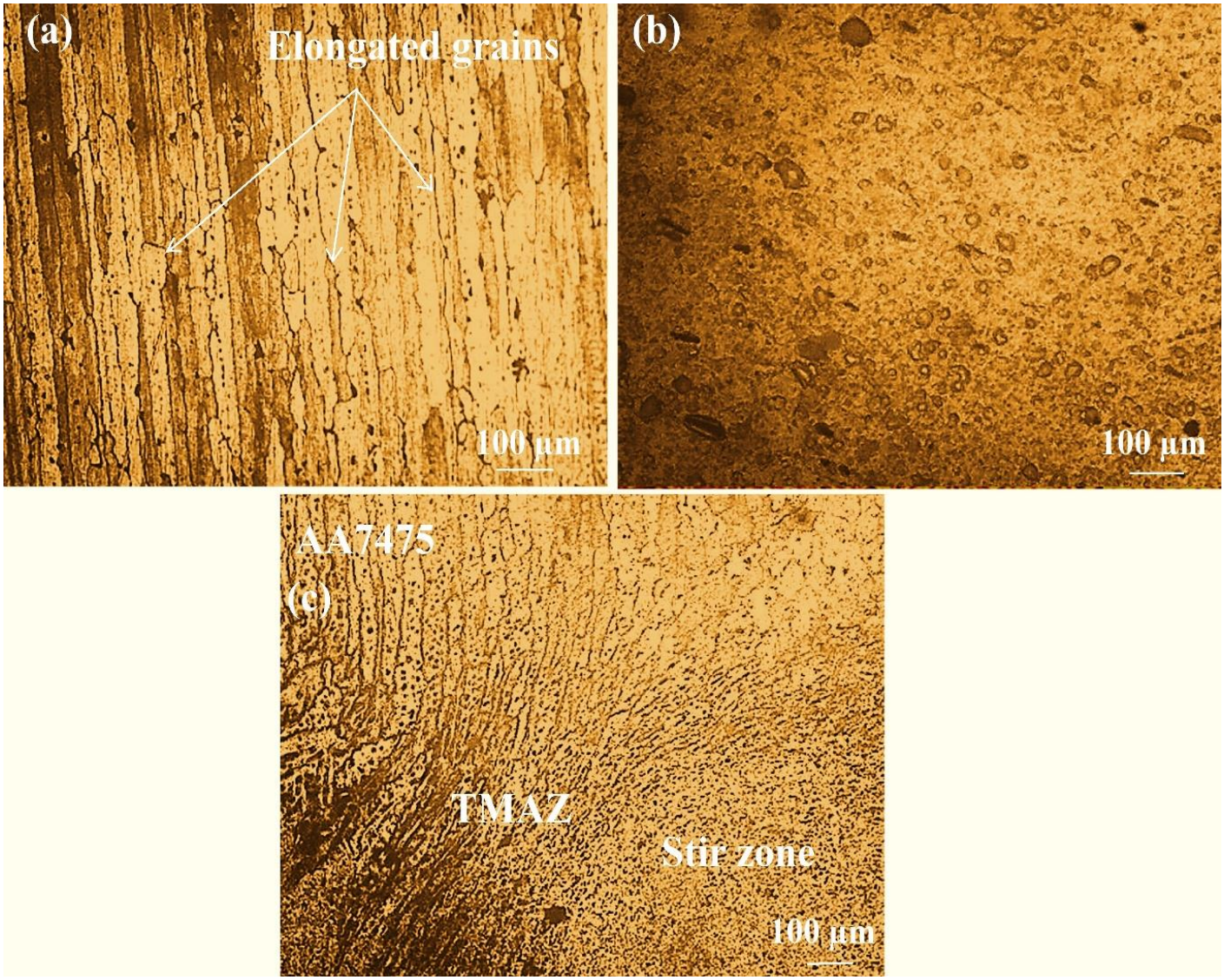

Figure 6: Optical images of base metal, (a) AA7475, (b) AA6061, (c) FSWed joint of AA7475 and AA6061

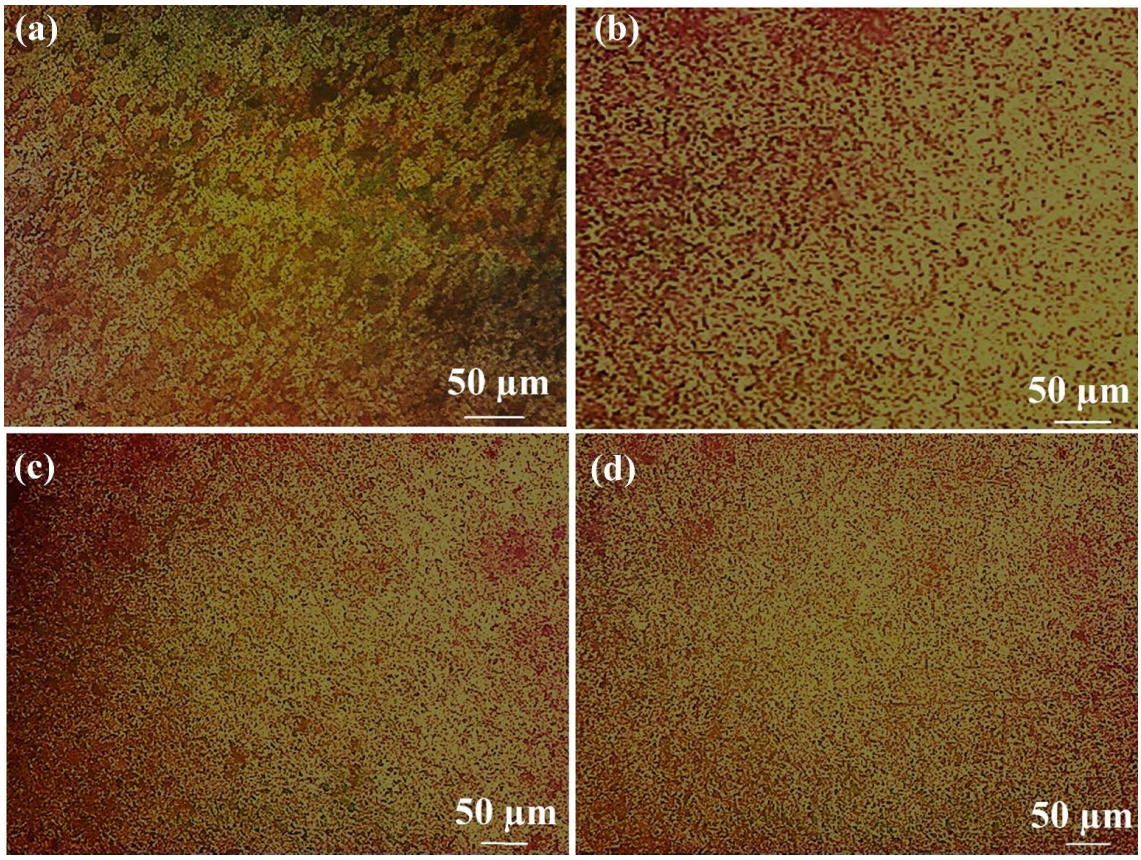

Figure 7: Optical images of FSWed joint of AA7475 and AA6061, (a) TRS 1000 rpm with TS of 120 mm/min, (b) TRS 1100 rpm with TS of 105 mm/min (c) TRS 1000 rpm with TS of 105 mm/min (d) 1200 rpm, TS of 105 mm/min

3.4 Fractography

The room temperature tensile fracture morphologies of the AA7475 and AA6061 reveals in fig. 8. At high magnification, there are many big dimples was observed in the fracture of the FSWed joints at low TRS, causing early fracture during the tensile test, whereas at high TRS fracture specimen, a lot of cleavage a lot of dimples was observed reveals in fig. 8. The FSWed fracture is constituted of several extremely small dimples with a small number of cleavage planes, signifying ductile-brittle hybrid fracture.

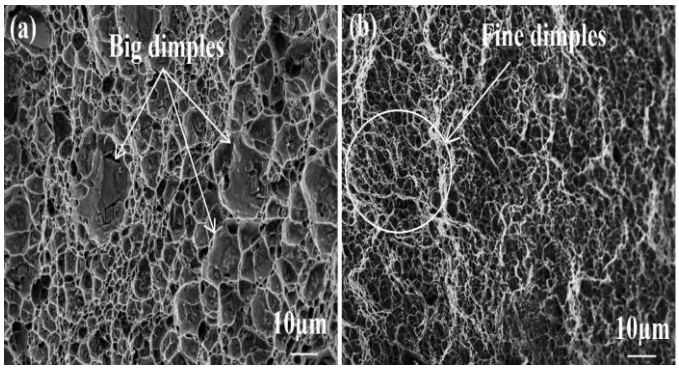

Figure 8 SEM images of tensile fractured specimen, (a) 1000 rpm, (b) 1200 rpm

4. Conclusions

The following conclusion have been made from the above investigation.

- AA7475 and AA6061 display strong plastic deformation at the SZ, leading in grain enhancement with a grain size of 9.2 µm at higher tool rotational speed and 21.52 µm at low rotational speed. Partially recrystallization was reported at the region of TMAZ due to inadequate distortion and lower temperature.
- The maximum tensile strength and the % strain at SZ were observed 247.41 MPa and 18.24%at TRS 1200 rpm and TS 105 mm/min, respectively, and the maximum hardness (127 HV) was observed in the SZ at TRS 1000 rpm and TS 90 mm/min.
- The grain size in the SZ was substantially finer with higher tool rotation than the lower tool rotation. The big and deep dimples can be seen in the FSWed part at 1000 rpm, whereas equiaxed fine dimples can be seen at TRS of 1200 rpm.

References

[1] Paidar M, Khodabandeh A, Najafi H, Sabour Rouh-aghdam A. An investigation on mechanical and metallurgical properties of 2024-T3

aluminum alloy spot friction welds. Int J Adv Manuf Technol. 2015;80(1):183.
[2] Paidar M, Khodabandeh A, Najafi H, Sabour Rouh-aghdam A. Effects of the tool rotational speed and shoulder penetration depth on mechanical properties and failure modes of friction stir spot welds of aluminum 2024-T3 sheets. J Mater Process Technol. 2014;28(12):4893.
[3] Husain Mehdi, R.S. Mishra, Analysis of Material Flow and Heat Transfer in Reverse Dual Rotation Friction Stir Welding: A Review, International Journal of Steel Structure, 19, 422–434 (2019).
[4] Motalleb-nejad P, Saeid T, Heidarzadeh Darzi AKh, Ashjari M. Effect of tool pin profile on microstructure and mechanical properties of friction stir welded AZ31B magnesium alloy. Mater Des. 2014;59:221.
[5] Paidar M, Sadeghi F, Najafi HR, Khodabandeh AR. Effect of pin and shoulder geometry on stir zone and mechanical properties of friction Stir spot-welded aluminum alloy 2024-T3 sheets. J Eng Mater Technol ASME. 2015;137(3):31004.
[6] Habibnia M, Shakeri M, Nourouzi S, Besharati Givi MK. Microstructural and mechanical properties of friction stir welded 5050 Al alloy and 304 stainless steel plates. Int J Adv Manuf Technol. 2014;76(5):819.
[7] Carlone P, Astarita A, Palazzo GS, Paradiso V, Squillace A. Microstructural aspects in Al–Cu dissimilar joining by FSW. Int J Adv Manuf Technol. 2015;79(5):1109.
[8] Guo JF, Chen HC, Sun CN, Bi G, Sun Z, Wei J. Friction stir welding of dissimilar materials between AA6061 and AA7075 Al alloys effects of process parameters. Mater Des. 2014;56:185.
[9] Husain Mehdi, R.S. Mishra, Microstructure and mechanical characterization of tungsten inert gas-welded joint of AA6061 and AA7075 by friction stir processing, Proceedings of the Institution of Mechanical Engineers, Part L: Journal of Materials: Design and Applications, 235 (11), 2531-2546 (2021). https://doi.org/10.1177/14644207211007882.
[10] Husain Mehdi, R.S. Mishra, Effect of Friction Stir Processing on Mechanical Properties and Wear Resistance of Tungsten Inert Gas Welded Joint of Dissimilar Aluminum Alloys. Journal of Material Engineering and Performance 30, 1926–1937 (2021).
[11] Husain Mehdi, R.S. Mishra, Influence of friction stir processing on weld temperature distribution and mechanical properties of TIG welded joint of AA6061 and AA7075, Transactions of the Indian Institute of Metals, 73, 1773–1788 (2020).
[12] Husain Mehdi, R.S. Mishra, Effect of friction stir processing on mechanical properties and heat transfer of TIG-welded joint of AA6061 and AA7075, Defence Technology 17 (3), 715-727, 2021 (2020).
[13] Husain Mehdi, R.S. Mishra, Effect of Friction Stir Processing on Microstructure and Mechanical Properties of TIG Welded Joint of AA6061 and AA7075, Metallography, Microstructure, and Analysis, 9, 403–418 (2020).
[14] Husain Mehdi, R.S. Mishra, Investigation of mechanical properties and heat transfer of welded joint of AA6061 and AA7075 using TIG+FSP welding approach, Journal of Advanced Joining Processes, 1, 100003, (2020) https://doi.org/10.1016/j.jajp.2020.100003.
[15] Husain Mehdi, R.S. Mishra, An experimental analysis and optimization of process parameters of AA6061 and AA7075 welded joint by TIG+FSP welding using RSM, Advances in Materials and Processing Technologies, 2020, https://doi.org/10.1080/2374068X.2020.1829952.
[16] P.A. Schweitzer, Aluminum and aluminum alloys, Met. Mater. Phys. Mech. Corros. Prop. (2003).
[17] B.T. Gibson, D.H. Lammlein, T.J. Prater, W.R. Longhurst, C.D. Cox, M.C. Ballun, et al., Friction stir welding: process, automation, and control, J. Manuf. Process 16 (2014) 56–73.
[18] K. Elangovan, V. Balasubramanian, Influences of tool pin profile and tool shoulder diameter on the formation of friction stir processing zone in AA6061 aluminium alloy, Mater. Des. 29 (2008) 362–373, http://dx.doi.org/10.1016/ j.matdes.2007.01.030.
[19] T. Dursun, C. Soutis, Recent developments in advanced aircraft aluminium alloys, Mater. Des. 56 (2014) 862–871, http://dx.doi.org/10.1016/ j.matdes.2013.12.002.
[20] Husain Mehdi, Arshad Mehmood, Ajay Chinchkar, Abdul Wahab Hashmi, Chandrabhanu Malla, Prabhujit Mohapatra, Optimization of process parameters on the mechanical properties of AA6061/Al2O3 nanocomposites fabricated by multi-pass friction stir processing, Materials Today: Proceedings, 2021. https://doi.org/10.1016/j.matpr.2021.11.333.
[21] A.H. Feng, D.L. Chen, Z.Y. Ma, Microstructure and low-cycle fatigue of a friction-stir-welded 6061 aluminum alloy, Metall. Mater. Trans. A 41 (2010) 2626–2641.
[22] M. Nourani, A.S. Milani, S. Yannacopoulos, Taguchi optimization of process parameters in friction stir welding of 6061 aluminum alloy: a review and case study, Engineering 2011 (2011) 144–155, http://dx.doi.org/10.4236/ eng.2011.32017.
[23] C.B. Fuller, M.W. Mahoney, M. Calabrese, L. Micona, Evolution of microstructure and mechanical properties in naturally aged 7050 and 7075 Al friction stir welds, Mater. Sci. Eng. A 527 (2010) 2233–2240.
[24] S. Rajakumar, C. Muralidharan, V. Balasubramanian, Establishing empirical relationships to predict grain size and tensile strength of friction stir welded AA 6061–T6 aluminium alloy joints, Trans. Nonferrous Met. Soc. China 20 (2010) 1863–1872.
[25] K. Elangovan, V. Balasubramanian, M. Valliappan, Effect of tool pin profile and tool rotational speed on mechanical properties of friction stir welded AA6061 aluminium alloy, Mater. Manuf. Process 23 (2008) 251–260.
[26] Husain Mehdi, R.S. Mishra, Study of the influence of friction stir processing on tungsten inert gas welding of different aluminum alloy. SN Applied Science, 1, 712 (2019). https://doi.org/10.1007/s42452-019-0712-0.
[27] Husain Mehdi, R.S. Mishra, Mechanical properties and microstructure studies in Friction Stir Welding (FSW) joints of dissimilar alloy- a review, Journal of Achievements in Materials and Manufacturing Engineering, 77 (1), 31-40, (2016).
[28] R. John, K.V. Jata, K. Sadananda, Residual stress effects on near-threshold fatigue crack growth in friction stir welds in aerospace alloys, Int. J. Fatigue 25 (2003) 939–948.
[29] R. Brown, W. Tang, A.P. Reynolds, Multi-pass friction stir welding in alloy 7050–T7451: effects on weld response variables and on weld properties, Mater. Sci. Eng. A 514 (2009) 115–121.
[30] Karthikeyan L, Senthil Kumar V S, Padmanabhan KA, On the role of process variables in the friction stir cast aluminum A319 alloy [J]. Materials & Design, 2010, 31(2): 761−771.
[31] Azimzadegan T, Serajzadeh S. An Investigation into microstructures and mechanical properties of AA7075-T6 during friction stir welding at relatively high rotational speeds [J]. Journal of Materials Engineering Performance, 2010, 19(9): 1256−1263.
[32] Abdellah Nait Salah, Sipokazi Mabuwa, Husain Mehdi, Velaphi Msomi, Mohammed Kaddami, Prabhujit Mohapatra, Effect of Multipass FSP on Si-rich TIG Welded Joint of Dissimilar Aluminum Alloys AA8011-H14 and AA5083-H321: EBSD and Microstructural Evolutions. Silicon (2022). https://doi.org/10.1007/s12633-022-01717-4.
[33] Several, P. and Jaiganesh,V.: A detailed investigation on the role of different Tool Geometry in Friction Stir Welding of various Metals & their Alloys, Proceedings of the International Colloquium on Materials, Manufacturing & Metrology – ICMMM, August 8- 9, pp 103 – 107, 2014.
[34] Husain Mehdi, R.S. Mishra, Consequence of reinforced SiC particles on microstructural and mechanical properties of AA6061 surface composites by multi-pass FSP, Journal of Adhesion Science and Technology, 2021, https://doi.org/10.1080/01694243.2021.1964846.
[35] Cavaliere, P., Squillace, A., 2005. High temperature deformation of friction stir processed AA7075 aluminum alloy. Mater. Charact. 55, 136–142.
[36] Mahoney M W, Rhodes C G, Flintoff J G, Spurling R A, Bingel W H, Properties of friction-stir-welded 7075 T651 aluminum [J]. Metallurgical and Materials Transactions A, 1998, 29: 1955−1964.
[37] Husain Mehdi, R.S. Mishra, Effect of multi-pass friction stir processing and SiC nanoparticles on microstructure and mechanical properties of AA6082-T6, Advances in Industrial and Manufacturing Engineering, 3, 100062 (2021). https://doi.org/10.1016/j.aime.2021.100062
[38] A.V. Strombeck, J.F.D. Santos, F. Torster, P. Laureano, M. Kocak, Fracture toughness behaviour of FSW joints on aluminum alloys, in: Proceedings of the First International Symposium on Friction Stir Welding, Paper No. S9-P1, California, USA, June 1999, TWI Ltd.

[39] A.Nait Salaha, Husain Mehdi, Arshad Mehmood, Abdul Wahab Hashmid, Chandrabhanu Malla, Ravi Kumar, Optimization of process parameters of friction stir welded joints of dissimilar aluminum alloys AA3003 and AA6061 by RSM, Materials Today: Proceedings, 2021, https://doi.org/10.1016/j.matpr.2021.10.288.

[40] H.J. Liu, H. Fujii, M. Maeda, K. Nogi, Tensile properties and fracture locations of friction-stir welded joints of 6061-T6 Aluminum alloy, J. Mater. Sci. Lett. 22 (2003).

Cite this article as: Vasim Abbas, Gaurav Kumar, Mukesh kumar, Effect of processing parameters on the microstructure and tensile properties of dissimilar aluminum alloys of AA7475 and AA6061, International journal of research in engineering and innovation (IJREI), vol 6, issue 1 (2022), 69-76. *https://doi.org/10.36037/IJREI.2022.6108*.